Application Note

Angle Measurement With Multi-Axis Linear Hall-Effect Sensors

TEXAS INSTRUMENTS

ABSTRACT

As the demand for automated precision control systems increases there is a similar increase to design systems that are more reliable and less likely to fail from mechanical wear. Many of these applications require the detection of angular rotation. While this function can be implemented using multiple one-dimensional sensors, a new class of three-dimensional sensors offers more flexibility and accuracy while allowing more compact designs.

Table of Contents

Trademarks

All trademarks are the property of their respective owners.

1 Introduction

Angular measurements are a critical form of system feedback for a wide array of applications. Precise rotational position may be calculated using Hall-effect sensors which will increase overall system reliability and success. When detecting the position of a robotic arm, the force applied to a foot pedal, or the position of a knob or level control, angular precision also improves overall system control for the end user.

1.1 Angle Measurement With One-Dimensional Sensors

A traditional approach to angular measurements using rotating magnets utilizes two linear Hall-effect sensors which are placed 90º apart in plane with a diametric cylinder magnet.
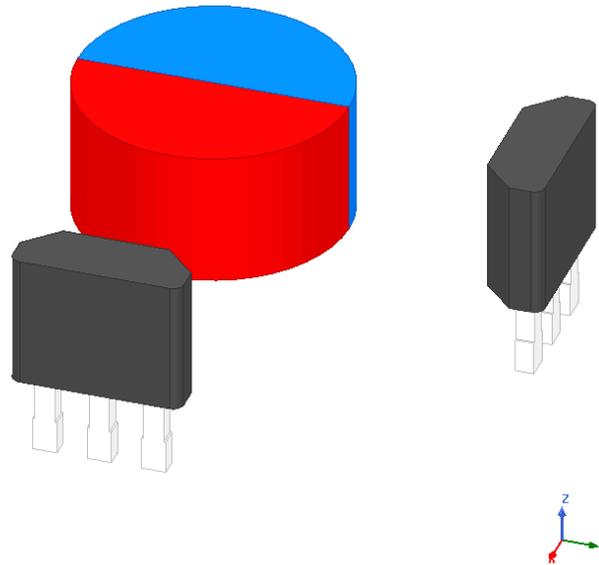

Figure 1-1. Two-Sensor Angle Measurement

A standard Hall-effect sensor is only capable of detecting the component of the magnetic flux density, or B-Field, which is normal to the face of the device. With the configuration in Figure 1-1, each sensor is detecting only the portion of the B-Field which is directed radially outward from the center of the magnet along one axis. As the magnet is rotated, the resulting outputs produce matched sine and cosine waveforms with a 90º offset which correlates to the physical placement. We can observe that the peak magnetic flux density each sensor detects occurs when the pole of the magnet is perfectly aligned toward that sensor.
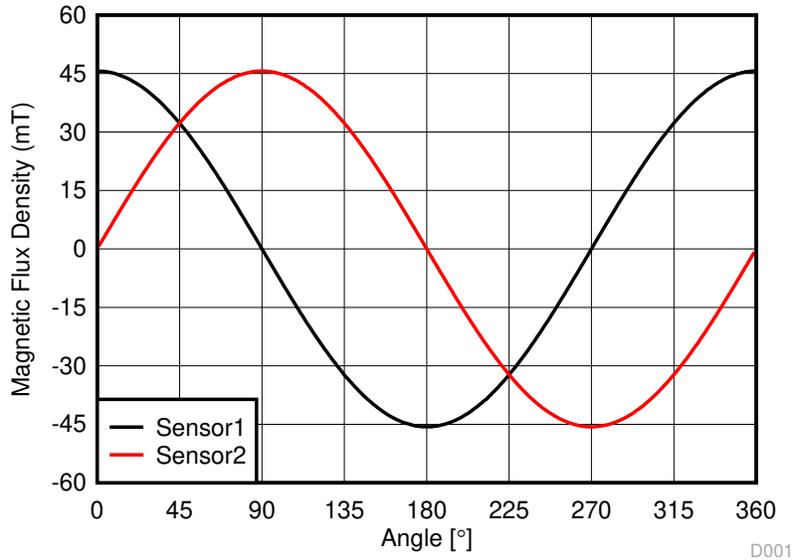
Figure 1-2. Two Sensor Input Signal

Given the trigonometric relationship of the outputs, the angle can be calculated by using the arctangent function. Specifically, the ATAN2 or ARCTAN2 function common in many math libraries is capable of accepting Cartesian (X,Y) inputs from all four quadrants and will calculate the associated angle.

This relationship provides a reliable method to determine the angle of rotating magnets. The *Linear Hall Effect Sensor Angle Measurement Theory, Implementation, and Calibration Application Report* is an additional resource that discusses this configuration in more detail.

1.2 Challenges of Angular Measurements

There are a few challenges that must be addressed when calculating the angle using two Hall-effect sensors.

Firstly, proper alignment requires enough PCB area to properly place both sensors at a reasonable distance from the magnet. Consider a NdFeB type magnet with a radius and thickness each of 3.125 mm (0.125 in).
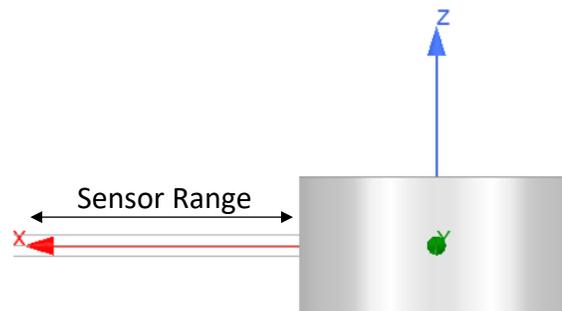

Figure 1-3. Example Magnet

We can analyze the observed input as the distance from the surface of the magnet to the sensor is varied, which is represented by "Sensor Range" in Figure 1-3. If the material grade of the magnet is also changed, we obtain a spacing profile for the various sensitivity options for any given sensor. Consider for example, a sensor with a peak input range of ±50 mT. Supposing a 10% buffer is provided to avoid risk of clamping the outputs, we obtain the field behavior shown in Figure 1-4.
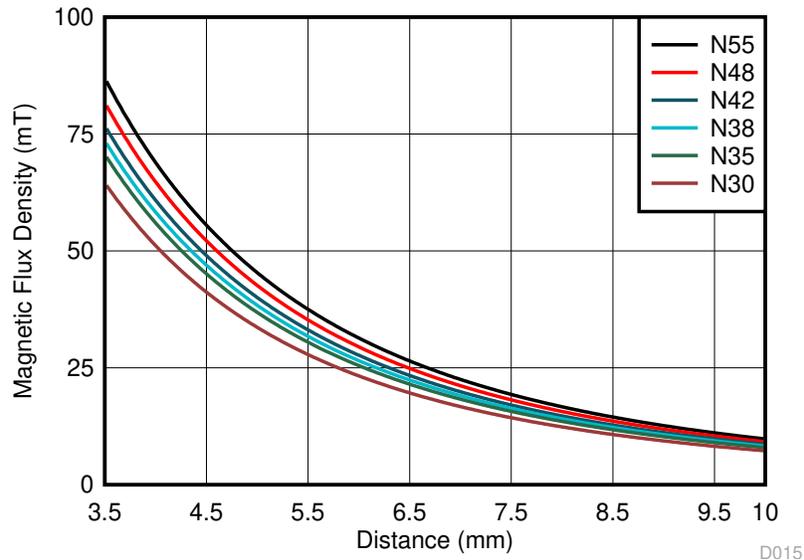
Figure 1-4. Magnetic Flux Density vs Distance for Various Magnet Materials

Notice the sensing range for the N35 magnet is 4.5 mm, whereas the N55 magnet has a target separation of 5 mm from the sensor. This distance will have a direct impact on the mechanics of the design within any target application. Any two-sensor solution will require enough physical space to place both sensors at the selected range. At this distance, even small changes in mechanical spacing can have a significant impact on the observed magnitude. Mismatch in spacing of the two sensors will lead to errors.

Secondly, it is important to account for device sensitivity variations. Consider a sensor with maximum sensitivity error of ±5%. In the worst-case scenario, one sensor will report a full scale output with 52.5 mT applied while the other reports with 47.5mT. When using the N35 magnet with an expected input of 45 mT, the output plots when rotating the magnet would appear as in Figure 1-5.
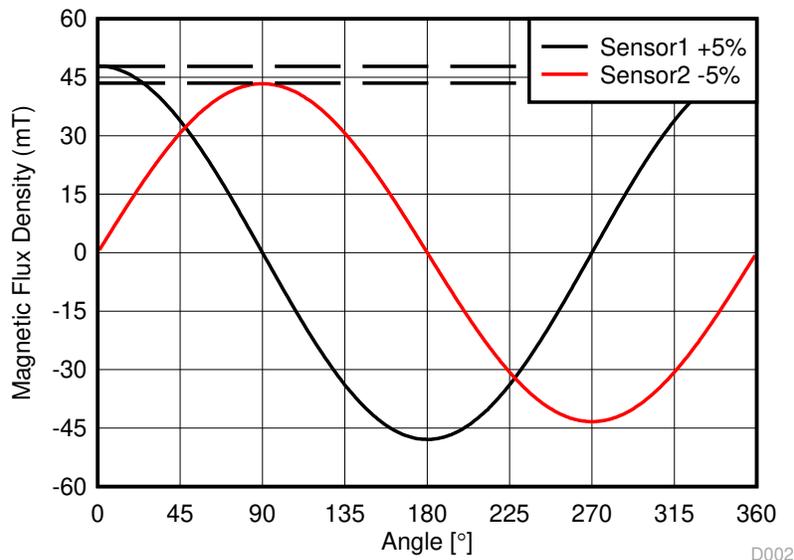

Figure 1-5. Detected Two Sensor Input with Sensor Mismatch

The angle error that results from this sensitivity error can be determined using the arctan calculation. Figure 1-6 shows a cyclically repeating error with a period of 180°. The minimum errors correspond to the zero crossings of either B-field input. In this instance, the peak angle error resulting from this sensitivity mismatch is 2.86º.
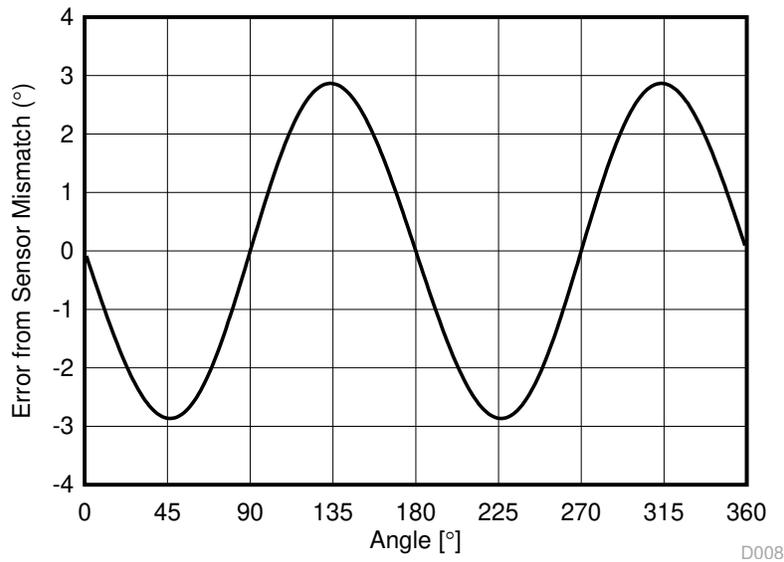
Figure 1-6. Calculated Angle Error From Sensor Mismatch

It is normal to expect in any system that there will be additional errors in magnet alignment and centering that may result in offset, wobble, or tilt. Alignment errors in assembly may impact the 90° spacing between sensors, or the physical assemblies may not be perfectly aligned. All manufacturing tolerances will have an impact on the system and it is expected to see additional errors that require calibration for optimal performance.

2 Benefit of Multi-Axis Sensors

A novel approach to minimize the challenges discussed related to one-dimensional (1D) sensors is to integrate multiple axes of sensitivity into a single device. In the example before, only a single component of the magnetic field was observed at each sensor.

Figure 2-1. 3D Sensor In Plane

If one sensor were to capture the X, Y, and Z components of the B-Field vector at the same location initially examined, we could reduce the device count and resolve uncertainty related to the mechanical assembly. Using just one such sensor at the same range as explored in the 1D case, we observe the fields shown in Figure 2-2.
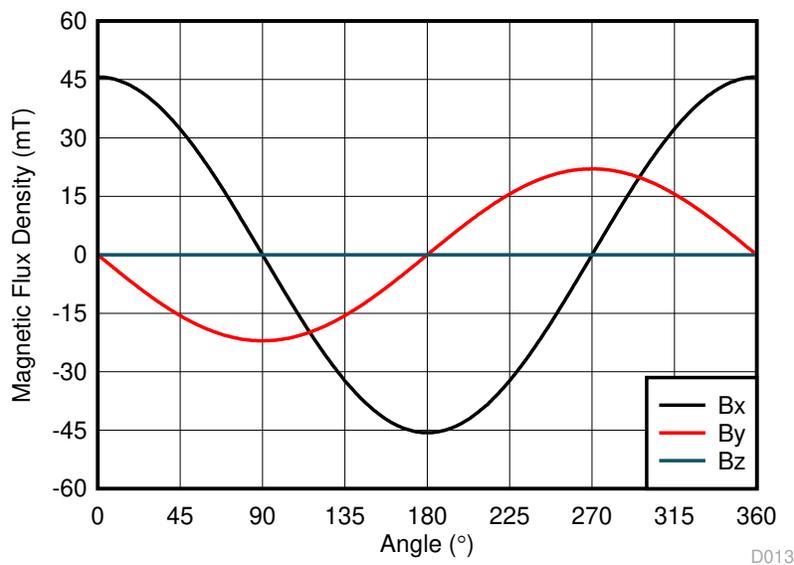
Figure 2-2. Magnetic Flux Density vs Angle for a 3D In-Plane Sensor

Notice in this position, the X and Y components again share a sine and cosine relationship. The Z component remains zero due to the sensor location being perfectly aligned to the magnet. Given the natural 90° phase shift between the X and Y inputs, a sensor with all three axes of sensitivity such as TMAG5170, makes a good candidate to detect the angular position of a rotating magnet regardless of package orientation. Alternatively, the TMAG5170D-Q1 is a dual-die version of the TMAG5170 that can be used if redundancy in the system is required.

As shown, the peak magnitudes are unequal, which we discussed to be a significant source of error in the two-sensor approach. Fortunately, the TMAG5170 device offers a simple solution to obtain peak matching which is explored in detail in this document.

2.1 Simplified Mechanical Placement

TMAG5170 device offers a wide degree of mechanical placement options. Typically, there are three primary configurations which are referred to as In-Plane, On-Axis, and Off-Axis.

In-Plane alignment, Figure 2-1, describes the configuration we have already shown where the sensor is aligned vertically to the center of the rotating magnet and is therefore placed coplanar with the magnet polarization.

On-Axis placement refers to the sensor being placed along the axis of rotation for a diametric magnet as shown in Figure 2-3. With the magnet rotating about the Z-axis, the sensor location could accordingly be placed along the Z-axis immediately above or below the magnet. The same air gap from the first example is maintained, but the displacement is downward in the Z-direction instead of outward in the Y-direction.
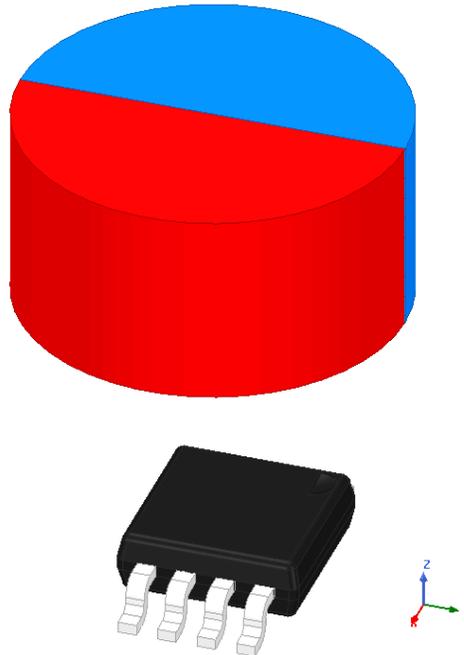

Figure 2-3. On-Axis Placement

Here the response for the X and Y components of the magnetic field are perfectly matched. This placement offers the easiest implementation for a multi-axis sensor as the inputs are naturally matched in amplitude and 90º out of phase.
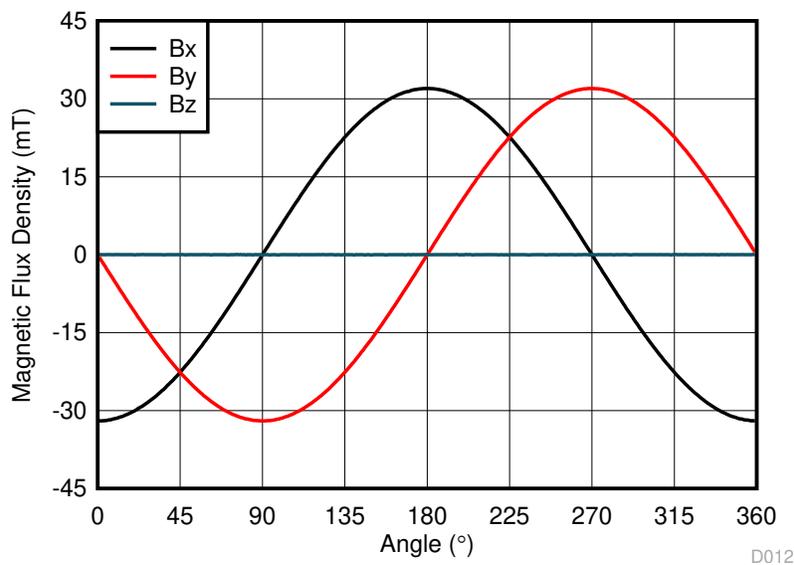

Figure 2-4. On-Axis Field Components

The last option is Off-Axis placement, which could be any other position within reasonable proximity of the magnet. For instance, suppose we continue to maintain the vertical air gap between the magnet and sensor, but

now move the sensor to a location directly beneath the outer circumference of the magnet as shown in Figure 2-5.
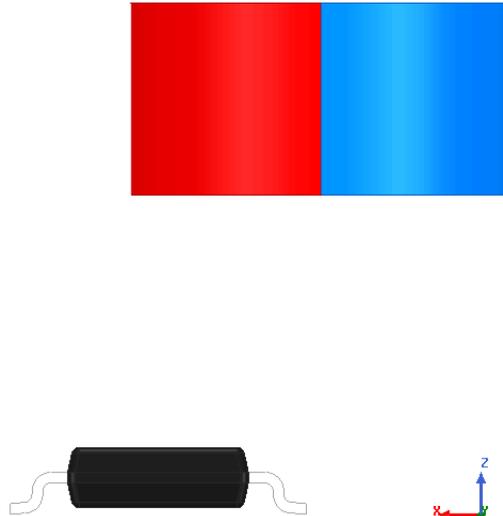

Figure 2-5. Off-Axis Placement

In this position we observe a portion of the magnetic field in each X, Y, and Z axes. Both the X and Z component of the field vector are 90° out of phase from the Y component.
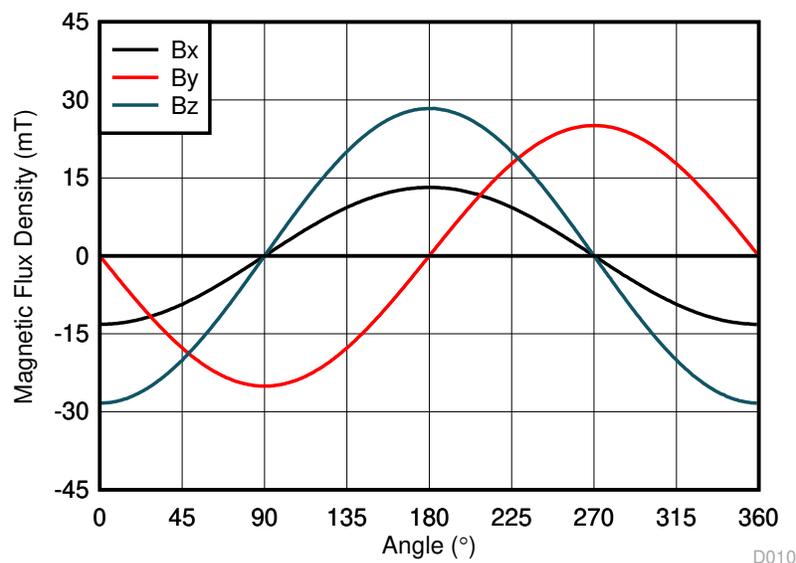

Figure 2-6. Off-Axis Field Components

Here it is best to select the Y and Z components of the magnetic field vector for angle calculations. These inputs will provide the greatest signal-to-noise ratio and are more closely matched than X and Y.

2.2 Sensitivity Matching

Whenever device sensitivity is matched such that each sensor produces equal amplitude outputs, the scenario shown in Figure 1-6 is resolved. For the greatest design flexibility, we need a way to achieve matching when using In-Plane and Off-Axis alignments. In each of these configurations, it is not uncommon to observe unequal peak amplitudes between the field components. Given this behavior, the use of these signals with the ATAN2 function will naturally exhibit an error similar to what is observed with a sensitivity mismatch. As the mismatch in amplitude increases, the severity of the angle error will likewise increase.

Hall elements in a single package undergo the same manufacturing and processes and it is reasonable to expect that the performance between any two sensors within the same device to be more naturally matched. However, even if the sensors were perfectly matched, we could still anticipate the error that results from unequal input magnitudes.

TMAG5170 solves this problem by allowing the user to normalize the calculation by attenuating the larger of the two inputs. For example, we can adjust the peak amplitudes seen in the In-Plane example such that the expected angle accuracy would only be limited by input referred noise and quantization error.
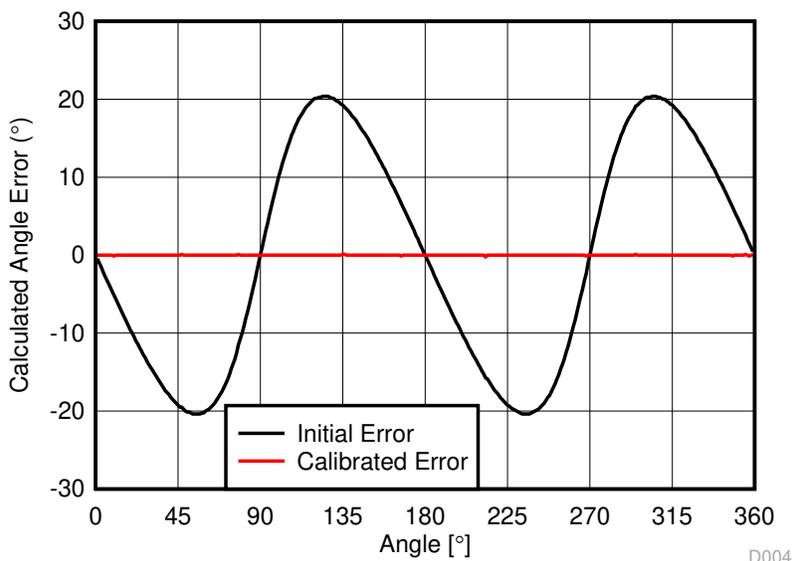

Figure 2-7. In-Plane Angle Error vs Input Correction

The ability to normalize the two outputs to each other makes TMAG5170 versatile in any angle sensing application.

2.3 CORDIC Angle Estimations

CORDIC, or *Co*ordinate *R*otation *Di*gital *C*alculator, provides a fast and effective way for digital systems to calculate angle using coordinate data. This algorithm quickly approximates angles by performing a binary search to rotate a point about the origin until the resulting vector lies along a single axis. As the coordinate input is rotated in iterative steps, the starting angle can be estimated by the summation of all steps. The resulting end position after completing these rotations will also produce the magnitude of the input vector. When used along with the outputs from a multi-axis Hall effect sensor, this algorithm proves to be an excellent option for fast and accurate angle calculations. Consider the point in Figure 2-8.
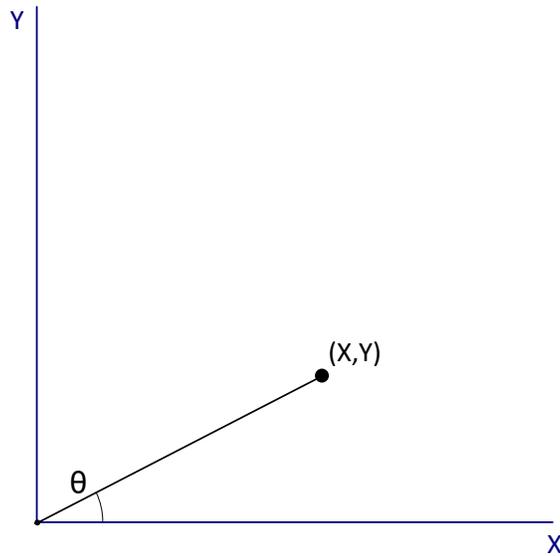
Figure 2-8. CORDIC Input

If this point is rotated 45° clockwise, denoted $\boldsymbol{\alpha_0}$, the new resulting vector leaves the first quadrant as Figure 2-9 shows.
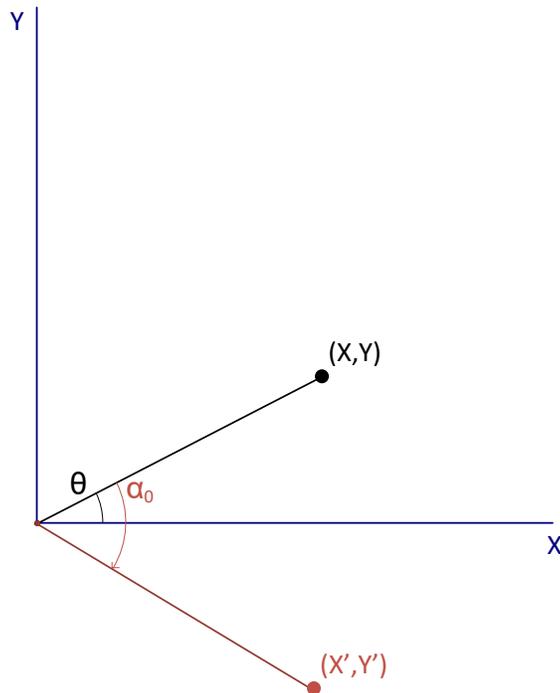

Figure 2-9. CORDIC First Step

Since the goal is to align the vector with the X axis, the direction of rotation must be adjusted counterclockwise in the next step. In the next iteration, the coordinate will be rotated counterclockwise by 22.5°, ($\boldsymbol{\alpha_1}$). The result here does not produce a quadrant change, and therefore the direction of rotation continues this direction. This process continues, adding and subtracting angular steps and changing rotation direction until the result is aligned to the X-axis. As shown in Figure 2-10, the approximate angle after 5 iterations is about 19.69°
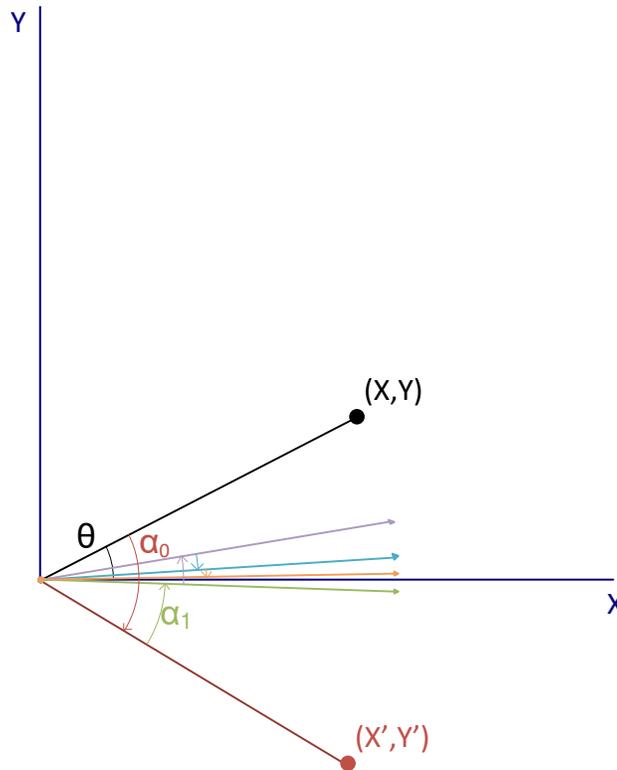
Figure 2-10. CORDIC - 5 Iterations

The algebraic process for rotating a coordinate point in space is described following the matrix multiplication in Equation 1.

$$\begin{bmatrix} x^{'} \\ y^{'} \end{bmatrix} = \begin{bmatrix} \cos(\alpha) & -\sin(\alpha) \\ \sin(\alpha) & \cos(\alpha) \end{bmatrix} \times \begin{bmatrix} x \\ y \end{bmatrix} \tag{1}$$

$$x^{'} = x\cos(\alpha) - y\sin(\alpha) \tag{2}$$

$$y^{'} = x\sin(\alpha) + y\cos(\alpha) \tag{3}$$

If **cos(α)** is factored from the resulting products, we are left with Equations 4 and 5 as a result:

$$x^{'} = \cos(\alpha) \times (x - y\tan(\alpha)) \tag{4}$$

$$y^{'} = \cos(\alpha) \times (y + x\tan(\alpha)) \tag{5}$$

As the algorithm progresses, we must determine the direction of rotation. If we were to choose to rotate counterclockwise instead, the result would produce Equations 6 and 7:

$$x^{'} = \cos(\alpha) \times (x + y\tan(\alpha)) \tag{6}$$

$$y^{'} = \cos(\alpha) \times (y - x\tan(\alpha)) \tag{7}$$

Notice that the only difference here is that the operation in each equation is inverted. Hence we can easily determine the direction of rotation by examining the sign of the operation. This rotation can be represented by a selectable value, which we will represent as **d**.

$$d_n = \begin{cases} 1 \ for \ CW \ rotation \\ -1 \ for \ CCW \ rotation \end{cases}$$

(8)

At this point a few approximations will simplify the angular calculation. If **cos(α)** were removed entirely, examination of the result would show that a new vector has been created which is rotated by the correct angle but has a magnitude greater than the original. This factor is effectively a scalar that normalizes the resulting vector to the correct magnitude for each step of the loop. The scalar value is determined by the angle of rotation, and can be easily calculated for each step by using a predetermined step size.

If a fixed number of iterations is used for every angle conversion, then the cumulative product of every vector transformation will always result with a constant final scalar, **m**. As a result, the value of **cos(α)** can be ignored during the routine. Instead, the final magnitude result can be scaled one time by **m**. Supposing ten iterations (0 to 9) of the algorithm were used, the resulting value for **m** is shown in Equation 9.

$$\frac{1}{m} = \prod_{n=0}^{i} \cos(\alpha_n)$$

(9)

$$m_9 = 1.64676$$

(10)

Additionally, we can note that **tan(α)** is close to the value of 2^{-n}. If the tangent calculation is replaced with a multiplication by a power of two, the algorithm becomes much simpler to implement. Consider the following table of values:

α_n [°]	$\tan(\alpha)$	2^{-n}	$\tan^{-1}(2^{-n})$ [°]
45	1	1	45
22.5	0.414	0.5	26.565
11.25	0.199	0.25	14.036
5.625	0.098	0.125	7.125
2.8125	0.049	0.0625	3.576

Since the resulting angle from this substitution is greater than or equal to the expected step value used in a true binary search, the new angular step size will still be able to converge. While one or two more iterations to achieve the same accuracy may be necessary, we gain the benefit of replacing a lookup table of tangent values with a fixed rightward bit-shift operation.

After implementing these modifications to the algorithm, we are left with Equation 11–Equation 14 which can be used iteratively to determine both the angle and magnitude of any two-dimensional vector.

$$x_{n+1} = x_n - y_n \times d_n \times 2^{-n}$$

(11)

$$y_{n+1} = y_n + x_n \times d_n \times 2^{-n}$$

(12)

$$\theta = \sum_{n=0}^{i} d_n \times \alpha_n$$

(13)

$$magnitude = \frac{x_i}{m}$$

(14)

Notice that with only a handful of cycles, this provides an elegant solution for a fast calculation. Devices with the CORDIC engine integrated, such as TMAG5170, are able to quickly resolve angular calculations and provide this as an output without any significant impact to overall conversion timing.

2.4 Tamper and Stray Field Detection

An added benefit of multiple axes of sensitivity is that tamper and stray field detection may be implemented. Again consider the outputs generated in the On-Axis placement.
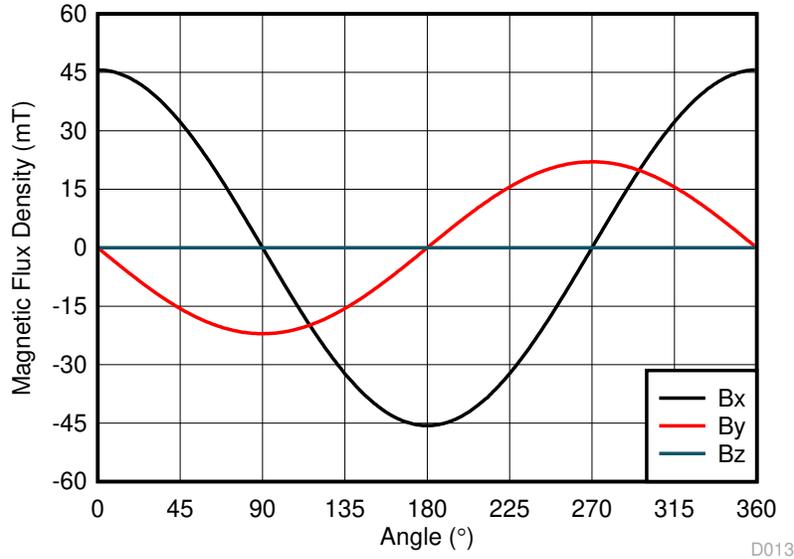

Figure 2-11. Magnetic Flux Density vs Angle for a 3D In-Plane Sensor

Notice in this case that while angle calculations are possible and only require the X and Y axes, that there is no input produced at this location in the Z direction. TMAG5170 allows the user to monitor all three axes together, and so with this configuration, any input on the Z-axis can indicate a magnetic field from an external source.

Additionally, TMAG5170 allows the user to programatically set thresholds for any axis that will trigger output on the ALRT pin. Both high and low thresholds may be set as Figure 2-12 shows.

Magnetic field crossing X_HI_THRESHOLD & X_LO_THRESHOLD levels

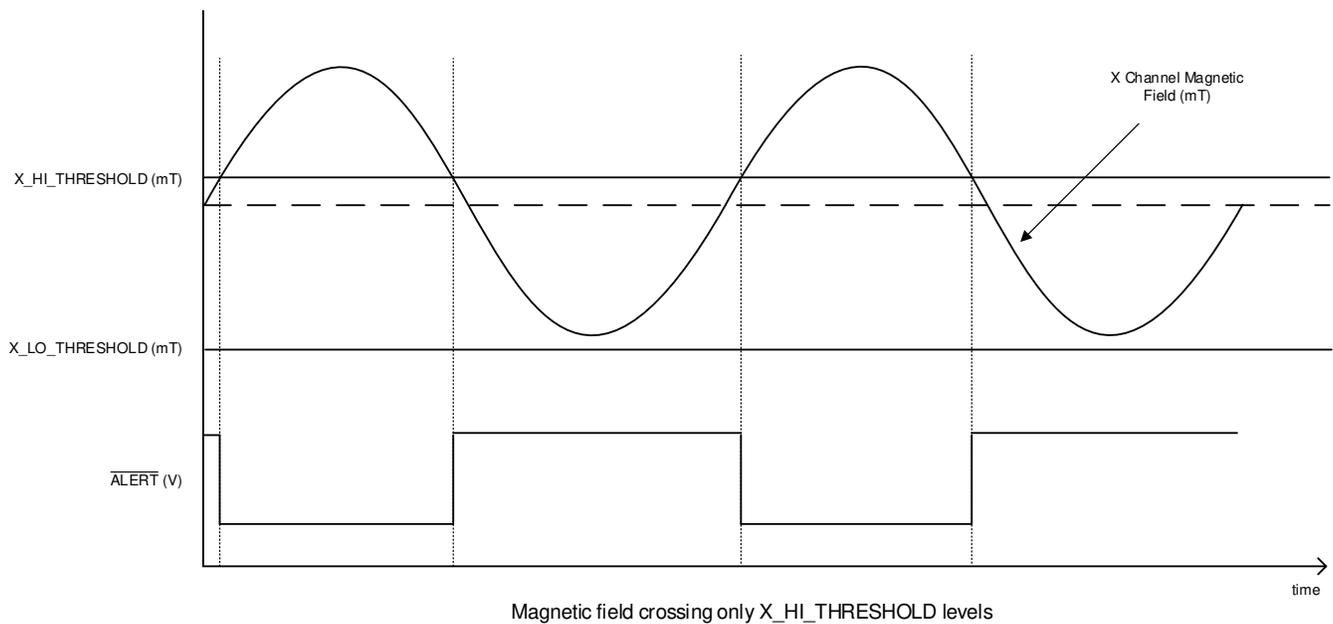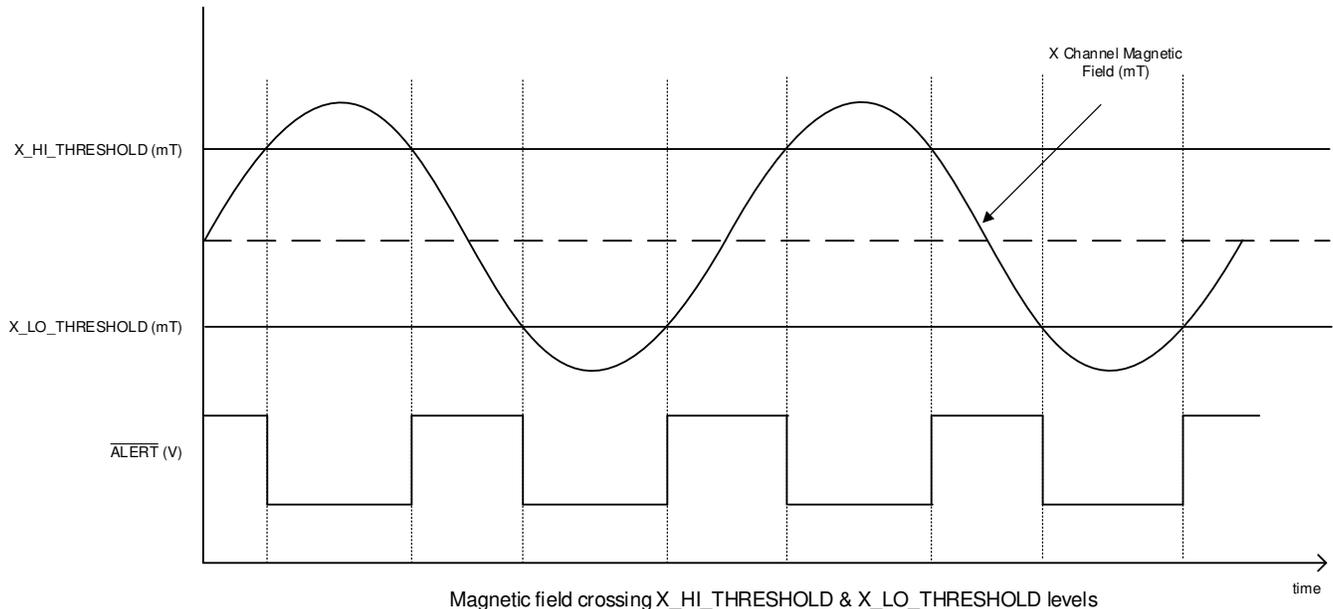Magnetic field crossing only X_HI_THRESHOLD levels

Figure 2-12. TMAG5170 Magnetic Switch Mode

Not only can a trigger be set on the unused axis, but we can set limits around acceptable inputs with the expected signals as well. Each axis may be independently programmed with both upper and lower limits. In this way the device may be configured to restrict operation to a fixed operating window for any magnetic input which should never be exceeded.

Adding this functionality to any measurement helps provide secure monitoring that may inform the controller when to take measures to prevent actions from false input.

3 Angular Measurement Considerations

Although multi-axis Hall effect sensors are able to simplify many of the problems related to capturing angular measurements, there are still a few important details to consider to which can help maximize performance.

3.1 Sensor Alignment

Having access to all three components of the B-Field vector greatly simplifies any placement with respect to the magnet. As previously discussed, the sensor may be placed anywhere near the magnet where there is significant enough magnetic flux density to be measured by scaling the outputs to a matched amplitude.

Despite this benefit, the rotational alignment of the sensor relative to the magnet is still worth considering. In many cases, the plane of the sensor will be constrained by the circuit board on which it is installed. Within this plane, the sensor will have freedom to rotate 360°. When placing the sensor either in-plane with the magnet or off-axis, the alignment of the sensor relative to the magnet will have an impact on the fields observed.

A sensor that is not aligned towards the center of a rotating magnet will separate the B-Field vector differently than shown in Figure 2-2. For instance, consider the alignment shown in Figure 3-1 with the sensor in-plane to the magnet.
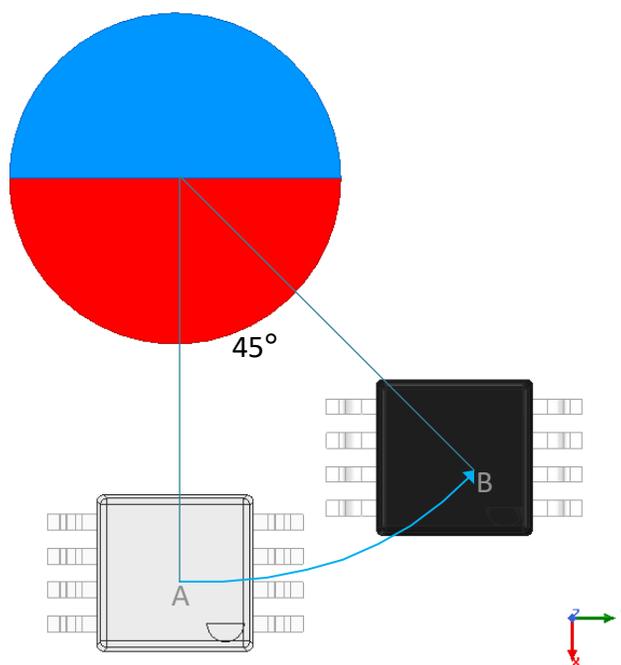

Figure 3-1. In-Plane Sensor With 45° Rotation

In this case, the sensor is at the 45° position, but is still aligned the same as when it was placed along the X axis. At 45° rotation of the magnet, the magnet pole is aimed at the sensor, but is not directly orthogonal to any element within the device. This can also be achieved by rotating the sensor in place by 45°. Mechanically, both orientations will produce the same effect. As a result of this rotation, we can observe the expected change to the magnetic field inputs in both positions A and B as shown in Figure 3-2.
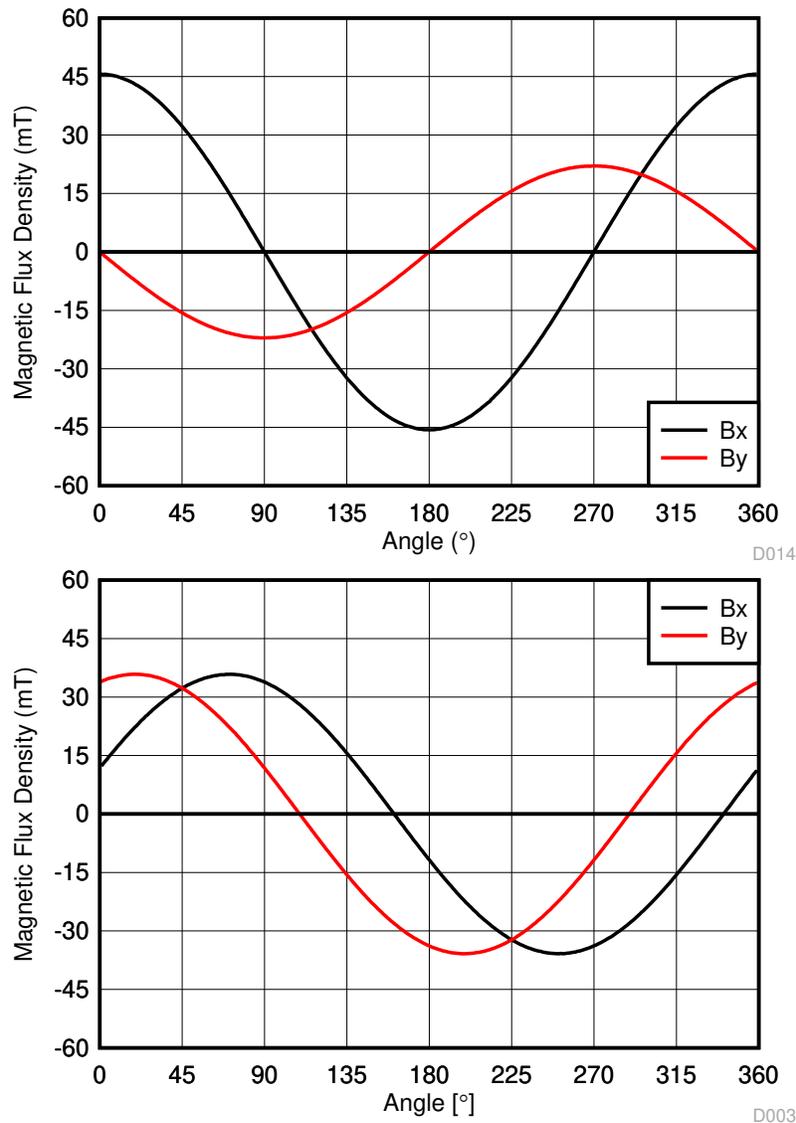
Figure 3-2. In-Plane Alignment with 45° Rotation

By rotating the sensor we have achieved matched inputs in each component of B-field vector. With the magnet rotated 45°, and with the pole directed towards the sensor, each Hall element will be matched relative to the X and Y components of the B-field vector and will detect magnitudes that are equal. With this rotation, each sensor is able to detect a peak value equivalent to the average of the original X and Y components of the B-Field vector. As a result, this orientation provides an ideal alignment of the magnet and sensor for In-Plane detection.

3.2 Sensor Calibration

In some systems, the sensor placement may be mechanically constrained such that neither 45° alignment In-Plane or On-Axis is possible. In these cases, sensor output matching will be necessary for optimal performance. Angular position calculations require that the components maintain a fixed magnitude throughout rotation to produce consistent results.

The circular shape of the magnet allows transcendental functions, sine and cosine, to describe angular changes in position. As long as both of these functions are scaled equally, the resulting calculated rotational path will be

circular. If the scaling of each component is unequal, the predicted path becomes elliptical. Angle error will be introduced by attributing an elliptical reference to a circular rotation (or movement).

To resolve this, the simplest method is to ensure the inputs to the CORDIC calculation are equal in magnitude. TMAG5170 device allows the user to adjust the CORDIC inputs by implementing a gain attenuation factor to any one channel.

Figure 3-3 illustrates a case where the amplitude of the X component, Ax, is greater than the amplitude of the Y component, Ay. Ax must be reduced to match the scale of Ay.
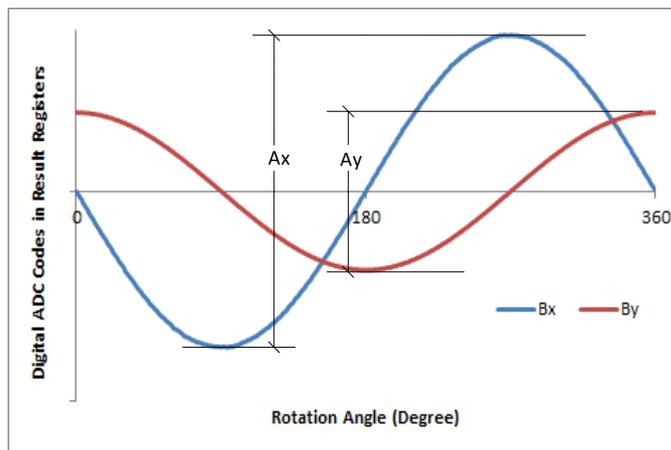

Figure 3-3. Magnitude Correction for Angular Calculations

The calibration process to set the peak values for TMAG5170 is simple:

1. Set the device to acquire the maximum number of samples per conversion by setting CONV_AVG register to 32x.
2. Rotate the magnet a full 360° rotation and record the output values for the axes of interest.
3. Determine the peak value for each axis
   a. Note which axis achieves the greatest magnitude input. Depending on sensor orientation and placement relative to the magnet, it is possible that this could be any of X, Y, or Z.
4. Calculate the gain adjustment: $$G_X = \frac{A_Y}{A_X}$$
   a. The ratio should always have the larger peak value on the denominator, such that G < 1. This axis will be attenuated by the Gain Factor, and is selected using GAIN_SELECTION register.
5. Multiply the Gain Factor, G, by 1024. Program the nearest integer value into the GAIN_VALUE register.

This feature allows the user to simultaneously correct for sensitivity mismatch and any error resulting from non-ideal alignment. Providing this correction allows the sensor to be placed anywhere near the magnet where two sufficiently large inputs are present.

3.3 Input Referred Noise

For any measurement system, it is important to remember the operating signal-to-noise ratio, SNR. In this case, the input referred noise of a Hall-effect sensor, will appear as a spurious magnetic field when observing the output. Ideally, this low level noise will be much smaller in magnitude than the actual input magnetic flux density.

As the input magnitude decreases, the signal-to-noise ratio will suffer, and the result will be less accurate angle measurements.

For many sensors, the only way to counter this effect is to use a stronger magnet or to place the sensor closer to the magnet. Cost and mechanical design may prohibit either of these options. TMAG5170 offers an additional means to reduce this noise further through averaged samples.

User-programmable averaging can be set at values ranging from 2× to 32×. While this does result in longer conversion times, it also allows for a reduction in the total effective noise. Each time the number of samples doubles, the effective RMS value of the input referred noise will scale down by a factor of √2. The benefit of

reduced input noise is of particular interest in cases where the input magnetic field is small. This option also can help reduce the impact of other external noise factors such as mechanical vibrations.

3.4 Impact of Sample Rate

Another variable to consider when designing a system that employs a 3D sensor for angle calculations is the sample rate of the sensor. For example, consider Table 3-1 which applies to TMAG5170.

Table 3-1. Update Rate Settings

OPERATING MODE	REGISTER SETTING	UPDATE RATE			COMMENT
		SINGLE AXIS	TWO AXIS	THREE AXIS	
X, Y, Z Axis	CONV_AVG = 000b	22.2 ksps	14.3 ksps	10.5 ksps	Fastest update rate
X, Y, Z Axis	CONV_AVG = 001b	14.3 ksps	8.3 ksps	5.9 ksps	
X, Y, Z Axis	CONV_AVG = 010b	8.3 ksps	4.5 ksps	3.1 ksps	
X, Y, Z Axis	CONV_AVG = 011b	4.5 ksps	2.4 ksps	1.6 ksps	
X, Y, Z Axis	CONV_AVG = 100b	2.4 ksps	1.2 ksps	0.8 ksps	
X, Y, Z Axis	CONV_AVG = 101b	1.2 ksps	0.6 ksps	0.4 ksps	Best SNR case

In the operating conditions presented in Table 3-1, the update rate for the various averaging modes is shown for one, two, or three axis operation.

In any system performing angle calculations on a moving target, the angular step between each measurement will be set by this sample rate. For instance, suppose TMAG5170 is sampling all three axes with the maximum averaging rate, or as we see in Table 3-1, 0.417 ksps. The time between each sample is about 2.4 milliseconds. If the magnet being sensed were rotating at 100 RPM, then the resulting angle change between each sample is 1.44 degrees. This will appear as a fixed offset in the measurement as well as define the minimum detectable change in angle.

Additionally, depending on the sample rate settings, there may be additional angle error. While operating in a pipelined fashion for the maximum sample rate, the typical conversion time for any TMAG5170 conversion is expected to be about 25 microseconds. If averaging 32 conversions, then the total sample time is about 800 microseconds. Over this time frame for the averaging of the first channel, the angle will have changed by 0.48 degrees. By the time the second channel conversion is complete, the angle will have increased by the same amount again for a total motion of about 1 degree. This offset in timing between the two samples will result in angle error. This again highlights the benefit of the pseudo-simultaneous sampling.

Care should be taken in systems where the magnet is rotating at high rates to account for these types of errors and select settings appropriately.

4 Practical Application

To help demonstrate this function, consider a few approaches to a simple rotary magnet which could be used in any number of applications, such as an e-shifter dial or a sensor attached to the motor of a robotic arm working in an automated factory. For this analysis we will attempt measurements using both an On-Axis and Off-Axis approach to demonstrate the design process.

4.1 Push-Button Knob

In conjunction with TMAG5170EVM, a push-button dial was designed to demonstrate the angle detection feature of the device. We will review the design procedure for this attachment which was implemented using the On-Axis approach.

4.1.1 Evaluating Design Constraints

To sufficiently demonstrate the performance of both the A1 and A2 variant of TMAG5170, it was determined that the input magnetic flux density should be close to full scale input for the highest range of the TMAG5170A1.

A knob with 1-in diameter was designed so that it could provide something substantial enough to manipulate while keeping the solution small enough to comfortably ship with the EVM packaging. As a result, the available opening for any magnet needed to be roughly 1/2 in.
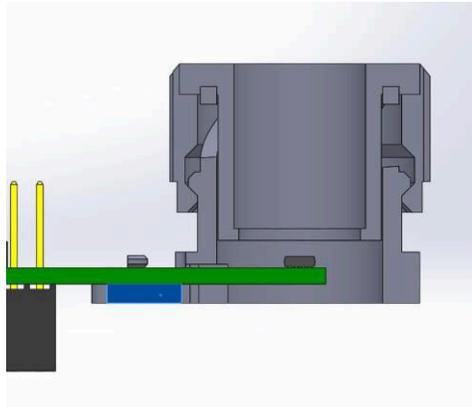
Figure 4-1. TMAG5170 Push-Button Knob Attachment

4.1.2 Magnet Selection

As previously mentioned, the magnet for the design needed to be 1/2 inch in diameter while providing enough magnetic flux density to operate near full scale input of the ±100 mT input range. It is best to leave headroom in the design to allow for variations, so a rough target of about 90% was chosen to guide magnet selection.

Even within this restriction, there is still a fair amount of flexibility regarding magnet thickness, magnet material, and the air gap between the magnet and sensor. For this diameter magnet, 1/8 in is a common available thickness that is available in multiple material types and is easily handled during assembly.

With a magnet geometry selected, simulations of magnetic flux density for various materials and air gaps were run to determine the remaining variables.
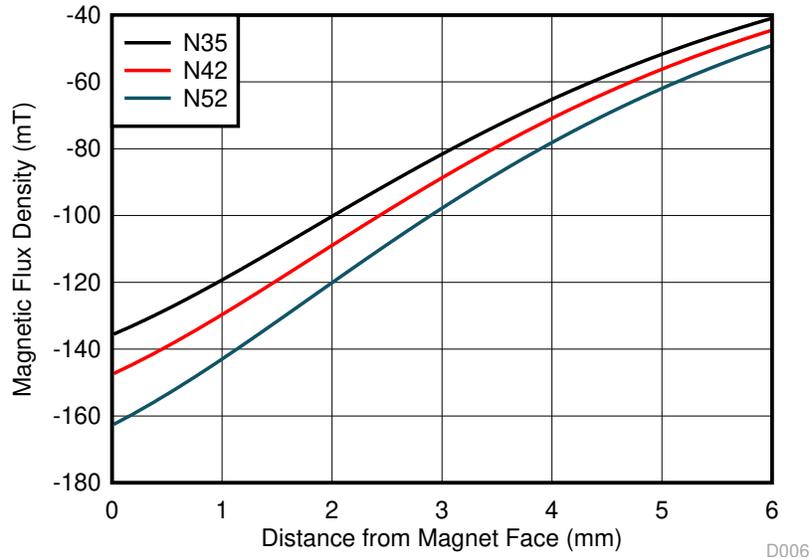
Figure 4-2. Push-Button Knob Proximity Simulation

Based on these results, the N42 material was selected to use at an distance of 3 mm from the sensor.

4.1.3 Prototyping and Verification

With the knob attachment mounted to the EVM, the GUI offers the option to capture and plot the outputs of each channel, or as an alternative, there is a visual interface which displays real time updates to the magnet angle.
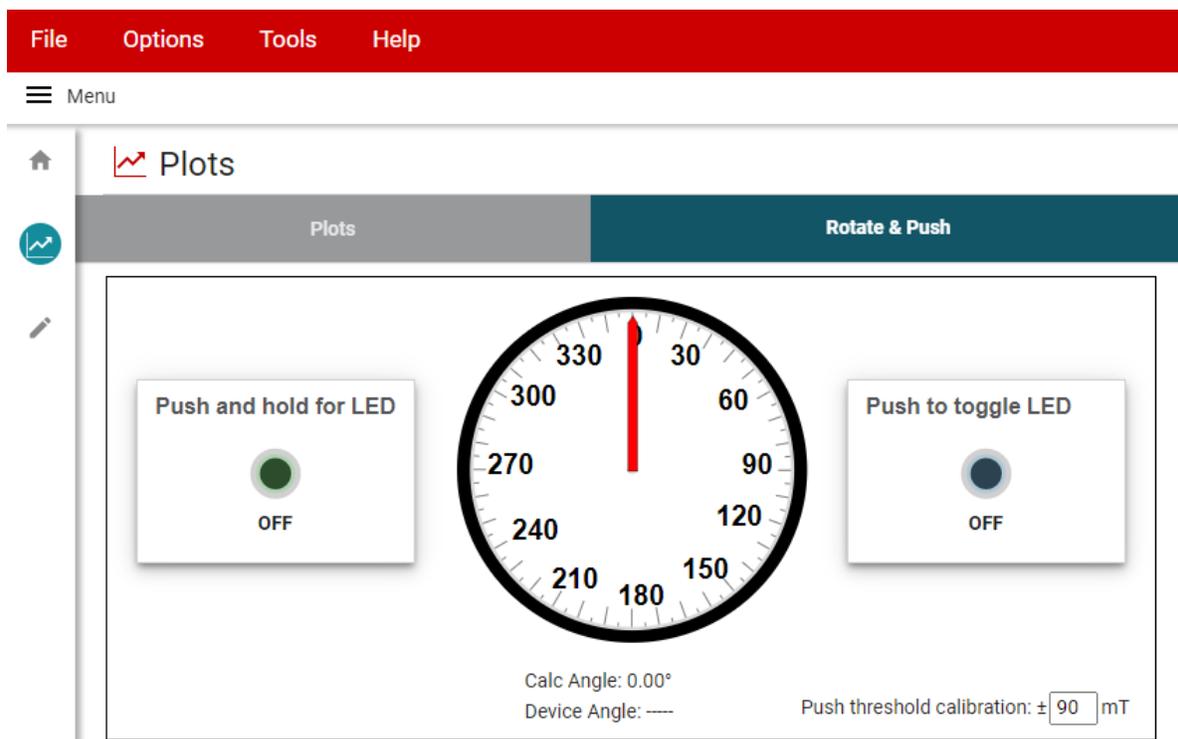

Figure 4-3. TMAG5170 Rotate & Push GUI

This output format helps to emulate the end application feel, but cannot tell us exact measurement errors.

Conversely, we can capture the data from a large number of data samples and then use this to plot of X and Y input data against the output angle. With this approach, we can look for anomalous behavior that would be indicative of any non-linearity in the angular response of the device.
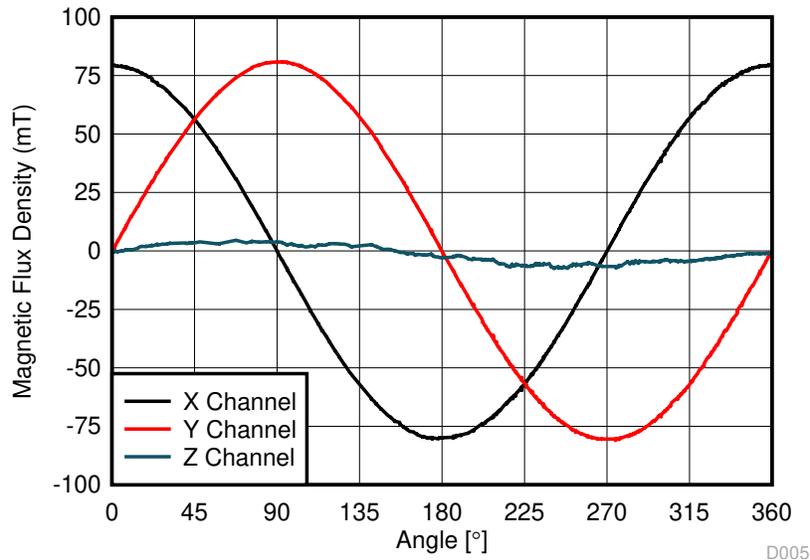
Figure 4-4. TMAG5170 Knob Attachment Measured Data

Notice here there are a few small irregularities, but over the course of a full rotation we see fairly smooth results that are very near to the pattern of the ideal input. This is primarily due to the handling of the knob impacting the sensor proximity and magnet tilt. There is also some offset which results with a detectable portion of the magnetic field in the Z-direction.

Also notice that the peak magnitude does not match the simulated value here. During the prototype build it was discovered that the spring used in the original knob design needed to be replaced, and that the replacement spring was somewhat ferromagnetic. Despite this interference, the end result is still capable of detecting a reasonably accurate angle for this use case. When designing any application, it is always recommended to consider the impact of external materials on the observed magnetic field.

4.2 Off-Axis Design

To further demonstrate the benefit of designing a system for angular measurement using a 3D sensor with sensitivity correction, we will also attempt an off axis configuration and measure the exact angle of the magnet as it rotates. For this effort, we want to place the sensor at the outer edge of the magnet similar to what is shown in Figure 2-5.

In this configuration, we will use the same magnet from the push-button knob, but will mount it to a motion controller that can accurately drive angular position. Here we can determine the exact performance of the configuration.

For this analysis, we will use the ±50 mT range and again target 90% full scale as a peak input value.

4.2.1 Sensitivity Gain Correction

Efforts with simulation software helped find an off-axis placement which resulted with a peak input in the Z-direction of approximately 45 mT. The same placement results in a peak magnitude of about 32 mT in the X-direction.
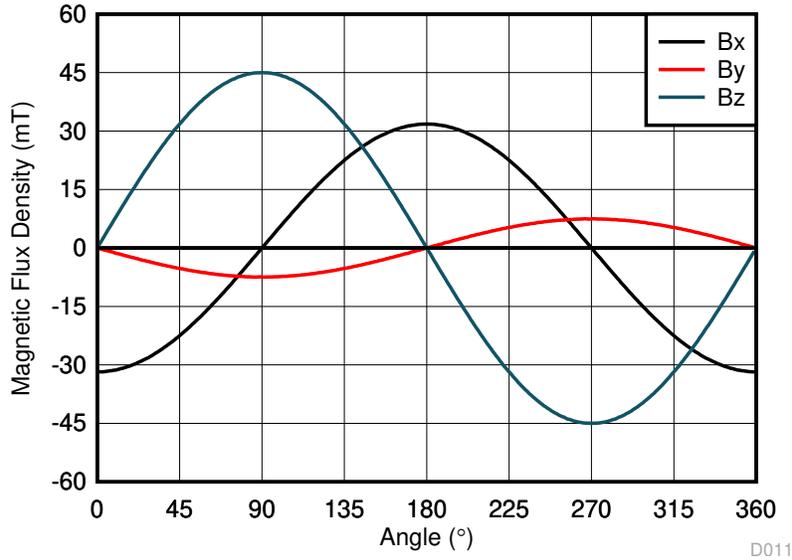

Figure 4-5. Simulated Off-Axis Configuration

This configuration was then matched in a physical setup and the outputs of a single rotation were captured. Here we see fairly close behavior between the X and Z components in the simulation and the captured results.
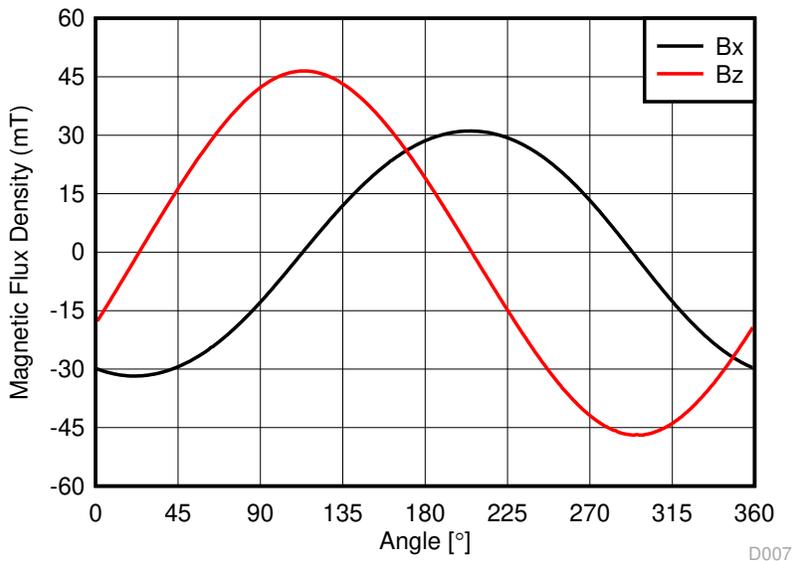
Figure 4-6. Initial Off-Axis Measured Data

To properly configure TMAG5170 for angular measurements it was necessary to attenuate the Z component to match the X component following the procedure detailed in Sensor Calibration. Based on measurements of peak input values, a scaling factor of 67.3% was determined to be required to match peak amplitudes.

4.2.2 Accuracy Verification

When performing angle calculations using the simulated data, the angle error is near zero for this approximate location and is negligible in comparison the 0.25 degree resolution of TMAG5170. While the initial measurement data shows outputs that appear to meet expectations and are sinusoidal in nature, we also find that when the angular position is calculated and plotted against the precise angular position that we see some unexpected angle error. This is represented as *Angle Error* in Figure 4-7.
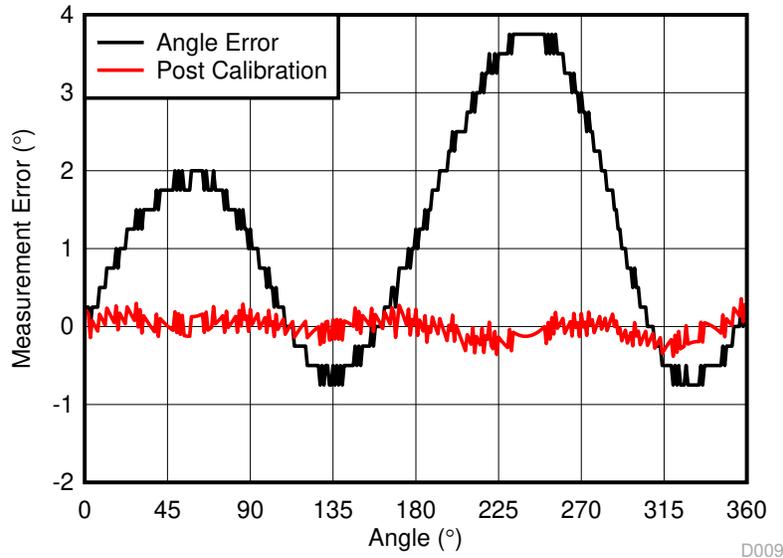
Figure 4-7. Measured Off-Axis Angle Error

The angle error observed in the physical setup, even after adjusting inputs for ideal matching, is related to mechanical errors in the setup. Minor amounts of magnet tilt and wobble have produced the cyclically repeating error.

There are a variety of approaches which might be used to further calibrate out this error, however. The *Linear Hall Effect Sensor Angle Measurement Theory, Implementation, and Calibration Application Report* discusses a variety of options which can be implemented to eliminate this behavior. The "post-calibration" curve in Figure 4-7 demonstrates the benefit of further calibrating measurements to achieve the most robust design possible. This can be essential in many applications where precision movement is mandatory such as is common in manufacturing and automation machinery.

5 Summary

Three dimensional sensors, such as TMAG5170, offer the ability to determine the angular position of a magnet using a single Hall-effect sensor. This is especially powerful in systems where space is limited. To help make the device even more accessible, built-in scalability allows the user to select nearly any position by allowing the system to scale inputs to the CORDIC calculator such that they are matched.

With amplitudes of input components matched, angular calculations are simple. The non-linearity of angular measurements can be easily eliminated by ensuring that the outputs are scaled to an equivalent magnitude before running the CORDIC algorithm.

Care should always be taken to account for mechanical tolerances and errors. The finest precision will always require some additional calibration as variations in magnet rotation such as tilt, wobble, and offset that occur during assembly and manufacturing are typically impossible to predict in advance.

6 References

- Texas Instruments, *TMAG5170-Q1 3-Axis Linear Hall Effect Sensor With SPI Interface Data Sheet*
- Texas Instruments, *TMAG5170D-Q1 Dual-Die High-Precision 3D Linear Hall-Effect Sensor With SPI Data Sheet*
- Texas Instruments, *TMAG5170UEVM Tool Folder*
- Texas Instruments, *TMAG5170DEVM Tool Folder*
- Texas Instruments, *Linear Hall Effect Sensor Angle Measurement Theory, Implementation, and Calibration Application Report*

7 Revision History

NOTE: Page numbers for previous revisions may differ from page numbers in the current version.

Changes from Revision * (January 2021) to Revision A (April 2023)   **Page**

- Added mention to the TMAG5170D-Q1.. 6
- Added references to the TMAG5170D-Q1 data sheet and the TMAG5170DEVM tool folder..........................24

Submit Document Feedback

IMPORTANT NOTICE AND DISCLAIMER